Çukurova Üniversitesi
Mühendislik Fakültesi Dergisi
Çukurova University
Journal of the Faculty of Engineering
ISSN: 2757-9255 CİLT/VOLUME: 40 SAYI/ISSUE: 1 MART/MARCH 2025

Experimental Investigation of Local Flexible Surface on Aerodynamic Effects for Finite Wing with NACA0018 Section

Ali Emirhan EROĞLU [1,a], **Tahir DURHASAN** [1,b], **Javad Rashid JAFARİ** [1,c], **İlyas KARASU** [2,d]

[1]*Adana Alparslan Turkes Science and Technology University, Department of Aerospace Engineering, Türkiye*
[2]*Samsun University, Department of Aerospace Engineering, Samsun, Türkiye*

[a]***ORCID**: 0009-0002-7006-2875; [b]**ORCID**: 0000-0001-5212-9170; [c]**ORCID**: 0009-0007-7497-7892; [d]**ORCID**: 0000-0003-3138-6236*

Article Info
Received : 02.01.2025
Accepted : 25.03.2025
DOI: 10.21605/cukurovaumfd.1665840

Corresponding Author
Tahir DURHASAN
tdurhasan@atu.edu.tr

Keywords
NACA0018
Flexible surface
Aerodynamic performance
Finite wing

***How to cite:** EROĞLU, A.E., DURHASAN, T., JAFARİ, J.R., KARASU, İ., (2025). Experimental Investigation of Local Flexible Surface on Aerodynamic Effects for Finite Wing with NACA0018 Section. Cukurova University, Journal of the Faculty of Engineering, 40(1), 61-68.*

ABSTRACT

The experimental study is conducted in low-speed wind tunnel in order to explore the effects of flexible surface on the aerodynamic performance of NACA0018 finite wing. In this purpose, lift and drag force of the wing measured using six axes load cell over the angle of attack 0°-18° at different Reynolds numbers. Moreover, surface oil flow visualization experiments are performed to depict the flow structure over wing. The flexible wing remarkably improves aerodynamic performance at $Re=3\times10^4$, and it also enhances the lift coefficient and diminishes the drag coefficient. The stall angle is delayed from 2.5° to 7°. It is observed that stall angle is shifted further angle of attack when Reynolds number increased. However, the effect of flexible surface on the aerodynamic performance diminishes with increasing Reynolds number. Furthermore, the observed tip vortex and laminar separation bubble significantly influence the surface flow structure.

NACA0018 Kesitli Sonlu Kanat için Yerel Esnek Yüzey Aerodinamik Etkilerinin Deneysel İncelenmesi

Makale Bilgileri
Geliş : 02.01.2025
Kabul : 25.03.2025
DOI: 10.21605/cukurovaumfd.1665840

Sorumlu Yazar
Tahir DURHASAN
tdurhasan@atu.edu.tr

Anahtar Kelimeler
NACA0018,
Esnek yüzey,
Aerodinamik perfomans,
Sonlu kanat

***Atıf şekli:** EROĞLU, A.E., DURHASAN, T., JAFARİ, J.R., KARASU, İ., (2025). NACA0018 Kesitli Sonlu Kanat için Yerel Esnek Yüzey Aerodinamik Etkilerinin Deneysel İncelenmesi. Çukurova Üniversitesi, Mühendislik Fakültesi Dergisi, 40(1), 61-68.*

ÖZ

Esnek yüzeyin NACA0018 sonlu kanat aerodinamik performansı üzerindeki etkisini araştırmak amacıyla düşük hızlı rüzgar tünelinde deneysel çalışma gerçekleştirilmiştir. Bu amaç doğrultusunda hücum açısının 0°-18° aralığında ve Reynolds sayısının farklı değerlerinde kanadın taşıma ve sürükleme kuvvetleri altı eksenli yük hücresi kullanılarak ölçülmüştür. Ayrıca, kanat üzerindeki akış yapısını resmetmek için yüzey yağ akış görselleştirme deneyleri gerçekleştirilmiştir. Esnek kanadın $Re=3\times10^4$'te aerodinamik performansı önemli ölçüde iyileştirdiği gözlemlenmiştir. Esnek yüzeyin taşıma katsayısını arttırmakla birlikte aynı zamanda sürükleme katsayısını da azalttığı bulunmuştur. Tutunma kaybı açısı 2,5°'den 7°'ye geciktirilmiştir. Reynolds sayısı arttığında tutunma kaybı açısının daha fazla hücum açısına ötelendiği gözlemlenmiştir. Bununla birlikte, esnek yüzeyin aerodinamik performans üzerindeki etkisi Reynolds arttıkça azalmaktadır. Ayrıca, gözlemlenen uç girdabı ve laminer ayrılma kabarcığının yüzey akış yapısı önemli ölçüde etkilemektedir.

1. INTRODUCTION

Recent advancements in aerodynamics have heightened interest in understanding the role of flexibility and fluid-structure interactions on the performance of an airfoil. Flexible wing designs, including morphing and membrane wings, have been identified as promising improvements to enhance lift and delay stall across various applications, from micro air vehicles (MAVs) to wind turbines [1,2]. The concept of partially flexible wings, which allows for static flexibility alterations, has aroused interest due to its potential to maintain optimal performance over diverse flight conditions. Despite these benefits, practical implementation remains challenging due to design complexity and material limitations [3,4].

Laminar separation bubbles (LSBs), often observed in low Reynolds (Re) number regimes, significantly impact aerodynamic performance by inducing separation, increasing drag, and reducing lift. Studies on both rigid and flexible airfoils have shown that flexibility can mitigate the negative effects of LSBs by suppressing separation and promoting reattachment. For instance, partially flexible membranes applied to airfoil surfaces have demonstrated improved lift-to-drag ratios and delayed stall angles. These findings underscore the importance of fluid-structure interaction in the development of advanced aerodynamic surfaces. Therefore, the advantages as well as the limitations of the flexible wings were thoroughly examined to reveal the size of LSB and the flow visualization downstream of the wing [5]. Also, Acikel and Genc [1] experimentally investigated the use of a partial flexible surface on the suction side of an airfoil to eliminate LSB at three different Re numbers. Even though they presented how the deformation and vibration mitigated the adverse effects of vortices such as producing improved lift and lower drag coefficients, the effectiveness of this method decreased with increasing Re numbers. At low Re numbers relevant to MAVs applications, Lian and Shyy [6] compared the performance of a rigid airfoil with a fully flexible suction surface. In their numerical study, they have demonstrated unsteady aerodynamic transitions at various angles of attacks by giving insights how the vibration of a flexible membrane would help prevent stall conditions. Since the ability of an airfoil to achieve higher lift is directly related to its geometrical structure, Yavuz [7] were numerically investigated the behaviors of both mechanical and aerodynamic performance of a free-formed airfoil, adapted from a NACA airfoil. The updated design effectively yields a better lift coefficient, additionally, for these cases, flow visualization with the help of surface oil visualization method provides insights into the flow phenomena, such as the vortex shedding mechanism as well as the presence of LSBs [8].

Moreover, the aeroelastic responses of flexible airfoils were examined in detail under various angles of attack and flow velocity conditions, with discussions addressing the associated flow phenomena [9] and the handling quality of the wing [10]. Kang et al. [11] and Lei et al. [12] numerically conducted 2D locally flexible surfaces to interpret the unsteady flow separation as well as the fluid-structure interaction. In their studies, the effects of flexibility and elastic stiffness on the lift generation were thoroughly investigated at low Re numbers. Their results reveal that optimal coupling between structural vibrations and vortex shedding frequencies can enhance lift through coherent vortex formation, while mismatched frequencies lead to irregular flow patterns and aerodynamic performance degradation. Additionally, the oscillation of the flexible surface generates downstream moving vortices and facilitates transport between the shear layer and the main flow, reducing separated regions and pressure on the upper surface. These mechanisms demonstrate the feasibility of flow control through flexible surface to improve lift. However, they stated that further research is required to address turbulence effects, low-aspect ratio configurations, and three-dimensional dynamics to advance the understanding of such systems. Boughou et al. [13] explored the fluid–structure interaction of hyperelastic morphing wing structures under low aerodynamic loads. The morphing wing consists of a rigid segment and a flexible segment, with the flexible portion occupies 60% of the chord length and constructed from a hyperelastic rubber-like material. The wing, with a flexible portion made of rubber-like material, shows enhanced efficiency at higher Re numbers and low angles of attack. These findings emphasize the potential of hyperelastic morphing wings for adaptive and efficient design applications. Similarly, Roy and Mukherjee [14] studied the aerodynamic performance of various wing sections (e.g., NACA0012, NACA4415, and NRELS809) to analyze the effects of morphing. Their investigation focused on pre- and post- stall angles of airfoils with flexible surface, comparing their performance to that of baseline airfoils. with the comparison of the baseline airfoils. In addition to passive control of fluid flow, He et al. [15] actively manipulated the suction surface of an airfoil utilizing a local flexible material driven by piezoelectric actuators that enhances the lift, and they also observed drag reduction at angles of attack (α) ranging between 10° and 14° in which the base airfoil experiences stall

under these conditions. By adjusting the actuation frequency, they achieved a maximum lift increase of 27.1% at angle of attack of 12°.

Furthermore, these types of flexible surfaces can be commonly used in wind turbine applications [16]. In Darrieus turbines, flexible profiles of NACA0018 and cambered Gö420 have been separately applied between rigid leading edge and trailing edges. This design accomplishes higher lift and torque coefficients, leading to significant gains in power output, especially at low tip-speed ratios, thereby addressing a key limitation of these turbines. Also, the low manufacturing cost demonstrates promising potential for efficiency enhancement with proposed design improvements to reduce drag. For SD7062 wind turbine airfoils, the flow transition from laminar to turbulence was thoroughly presented [17]. The formation of LSB was observed at α=8° for the specific location of the chord length. However, the flow structure transformed to a turbulent region because of reattachment of the flow when the locally flexible surface applied. Additionally, the stall angle was postponed from 10° to 12° compared to the baseline case.

Even though flexible surfaces on airfoils are available in the literature, the focus has predominantly been on infinite wing. However, their potential for finite wing remains underexplored. This study aims to further investigate the effects of finite wing flexibility on aerodynamic performance via experimental analysis. By focusing on low Reynolds number flows, this study explores how flexible surface deformation interacts with fluid flow to enhance aerodynamic efficiency, contributing to the advancement in modern aeronautics, such as adaptive morphing wing designs for MAV applications. Experiments were conducted on a NACA0018 finite wing by applying locally flexible surfaces to both sides of the wing for 3×10^4 and 10×10^4 of Re numbers based on chord length. Based on the results, it was shown that integrating flexible surfaces can result in effective flow control.

2. MATERIAL AND METHOD

The experiments were conducted in a suction type and low-speed wind tunnel in the Aerodynamic Laboratory of the Department of Aerospace Engineering at the University of Adana Alparslan Türkeş Science and Technology. The wind tunnel has a square test section with a dimension of 600mm×600mm, surrounded with a transparent plexiglass wall for observation of the flow phenomena. The tunnel could run at the maximum speed of 20 m/s. The turbulence intensity in the tunnel test section is less than 1 % for this study. Figure 1 schematically illustrates the experimental setup, including the airfoil with a servo motor for adjusting its angles of attack and a six-axis load cell for measuring the forces acting on the airfoil.

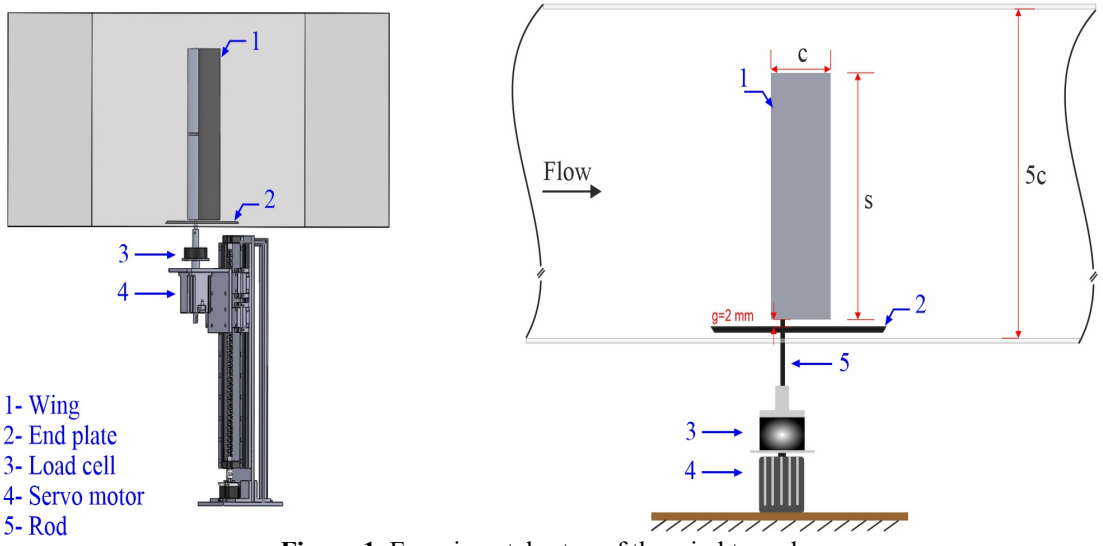

Figure 1. Experimental setup of the wind tunnel

NACA 0018 finite wing model was used in the present study. The chord length (c) was 120 mm, and span length (s) was 480 mm, corresponding to an aspect ratio of 4. The design and fabricating processes of the partially flexible NACA0018 airfoil were presented in Figure 2. The position of flexible membrane material was identified from x/c=0.35 to x/c=0.85 since laminar separation bubble dominate in that region for the

rigid NACA0018 airfoil at moderate angle of attack. The flexible membrane was supported by a rib having a thickness of 0.0125s in the middle of the span. After the design processes, airfoils were produced by a 3D printer. The produced airfoil was rubbered via sandpaper to prevent the roughness effect of the solid surface. The flexible material used in this study was a 0.2 mm latex rubber sheet having Young's modulus of 2.2 MPa. The flexible membrane was attached to the frames over the airfoil by using 0.05 mm thin double-sided tape.

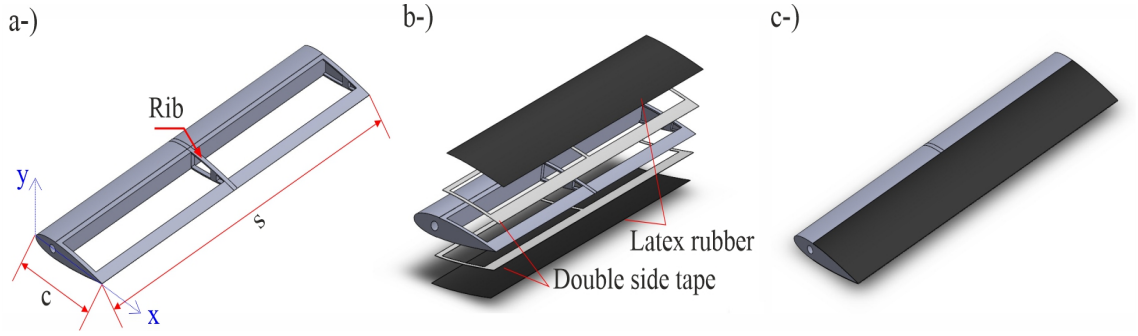

Figure 2. NACA0018 airfoil: (a) without flexible materials (b) fabricating process and (c) final product with partial flexible surfaces

Aerodynamic force measurements were conducted at two different Reynolds (Re) numbers based on chord length 3×10^4 and 10×10^4. Lift and drag force data were collected using six-axis load cell at a sampling rate of 1000 Hz over a time interval of 20 s for all cases. Force measurement system has accuracy of 0.5% of full scale. Experiments were performed at angle of attack between 0° and 18°. After lift (F_L) and drag (F_D) forces were obtained, it has calculated the dimensionless coefficients of lift (C_L) and drag (C_D) in conjunction with Equation 1 and 2.

$$C_L = \frac{F_L}{0.5\rho U_\infty^2 A} \tag{1}$$

$$C_D = \frac{F_D}{0.5\rho U_\infty^2 A} \tag{2}$$

where ρ, U_∞, and A denote the density of air, free-stream velocity, and projection area of the airfoil.

Surface oil visualization were carried out to reveal the effect of laminar separation bubble and tip vortex on the upper surface flow characteristic at angle of attack α=4°, 8° and 12°. The surface oil visualization is based on the painted matte black wing surface by pigmented oil and then dried via flow to obtain a flow pattern. The mixture consists of kerosene, titanium dioxide and a very small amount of oleic acid.

3. RESULTS AND DISCUSSION

Surface oil visualization over rigid finite wing is presented in Figure 3 in order to depict the effect of laminar separation bubble and tip vortex on the flow structure at angle of attack of α=4°, 8° and 12°. It is seen that the boundary layer separated approximately at x/c=0.2 and then reached at x/c=0.5. The dense pigment area between the separation (LS) and reattached (R) point indicates the formation of a laminar separation bubble (LSB). It is also observed that trailing edge separation (TS) occurs at x/c= 0.8. The tip vortex directs the flow inwards and creates a chaotic flow structure marked by the dashed turquoise line in this figure. Moreover, it affects the LSB over the wing. As the angle of attack increases from 4° to 8°, the separation and reattachment points shift closer to the leading edge, and the size of the laminar separation bubble decreases. At α=12°, separated boundary layer is not reattached, so stall occurs. Furthermore, the tip vortex enlarges, shifts inward along the wing, and becomes more dominant in shaping the upper surface flow structure as the angle of attack increases. Oil visualization experiments were not performed at 3×10^4 because the momentum of the flow was too low to sweep away the oil mixture.

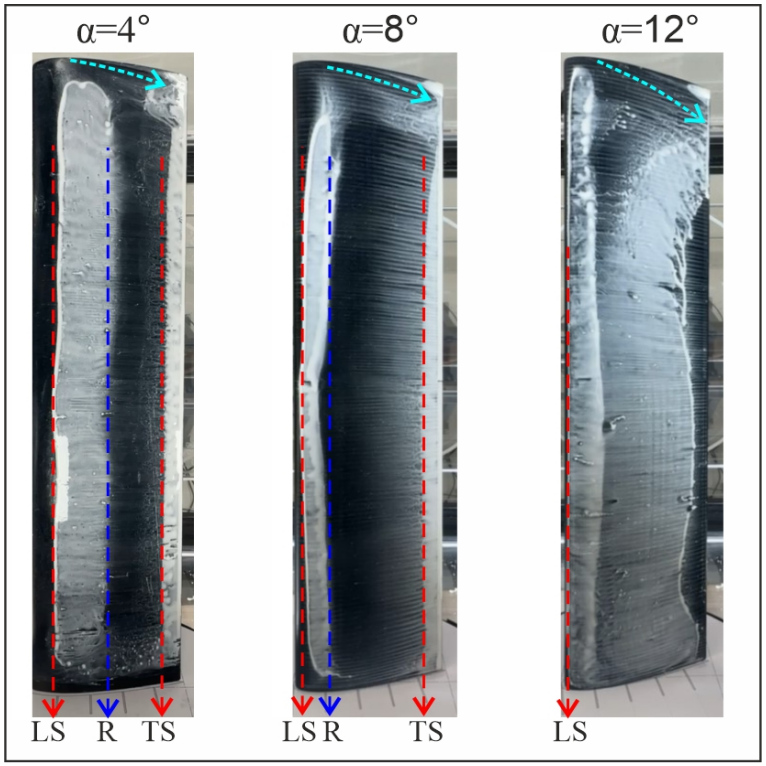

Figure 3. Oil flow visualization over rigid finite wing at Re=10×10^4

The effect of flexibility on the mean lift coefficient (C_L) of NACA0018 finite wing is shown in Figure 4 at Reynolds number of Re=3×10^4 and 10×10^4. The C_L variation for rigid NACA 0018 finite wing is also presented in order to constitute as a reference. At angle of attack α=0°, the value of C_L is zero for all cases due to symmetrical wing. At Re=3×10^4, the rigid wing generates lift force when the angle of attack is increased from 0° to 2° (Figure 4a). However, the rise in C_L is observed only up to the angle of attack α=2.5°. Beyond this angle of attack, the variation of C_L with the angle of attack indicates formation of smooth stall for rigid wing. On the other hand, the C_L distribution of the flexible membrane wing is substantially different from that of its rigid equivalent. It is clearly seen that flexible wing significantly postpones the stall angle in comparison with rigid wing at Re=3×10^4. The C_L remarkably increases with the increasing angle of attack and reaches its maximum value at α=7°. A sudden decrease in C_L at α=8° indicates the formation of abrupt stall for flexible wing. Figure 4b compares C_L of rigid and flexible wings at Re= 10×10^4. It is observed that Reynolds number significantly effective on the C_L distribution. The lift curves display nearly linear variation at moderate angles of attack for both wings. The stall angle and also maximum C_L are significantly enhanced when Reynold number is increased from 3×10^4 to 10×10^5 for rigid and flexible wings. The maximum C_L is obtained at α=11° and 11.5° for rigid and flexible wing, respectively. Furthermore, flexible wing shows abrupt stall behavior at Re=10×10^4 on the contrary to Re=3×10^4. On the other hand, the flexible wing has insignificant effect on the C_L in comparison with rigid wing at Re= 10×10^4. Similar trend is also observed by Genc et. al (2020). They demonstrated that the effect of flexibility on the aerodynamic performance of NACA4412 decreases with increasing Reynolds number and it behaves like a rigid wing at Re=7.5×10^4. It should be pointed out that the flexible wing exhibits higher performance on C_L in the post-stall region at Re=3×10^4 and 10×10^4 when compared to the rigid wing.

The distribution of drag coefficient (C_D) for rigid and flexible wings at Re=3×10^4 and 10×10^4 are depicted in Figure 5. It is seen that the flexibility is not only effective on the C_L but also on the C_D. Furthermore, flexible wing exhibits different behavior in pre and post stall regions when compared to the rigid wing. It is observed that at the Re=3×10^4, flexible wing has a significantly lower drag than the rigid wing (Figure 5a) up to α=7°. On the other hand, in the post stall region, the flexible wing has remarkably higher drag than the rigid wing. As the Reynolds number is increased, drag coefficient of flexible wing is nearly same with rigid wing up to stall angle (Figure 5b). However, C_D of flexible wing is greater than rigid wing in the post stall region.

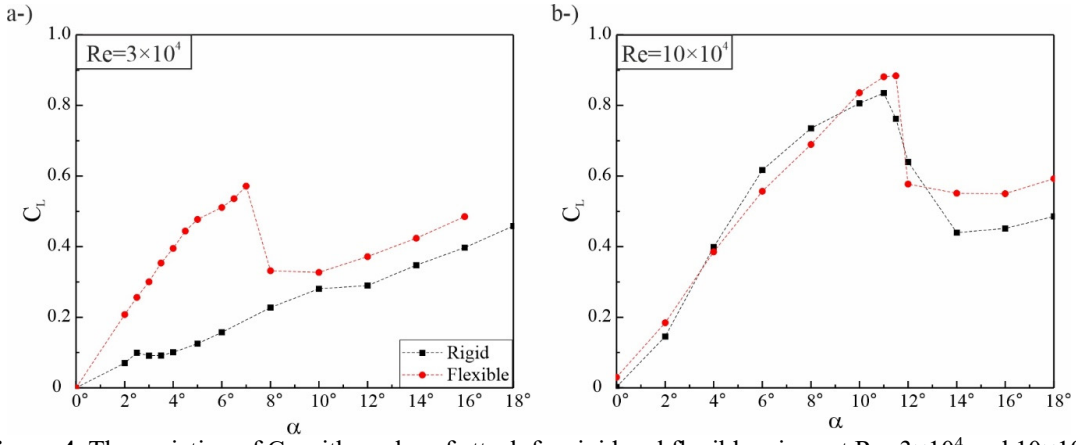

Figure 4. The variation of C_L with angles of attack for rigid and flexible wings at Re=3×10^4 and 10×10^4.

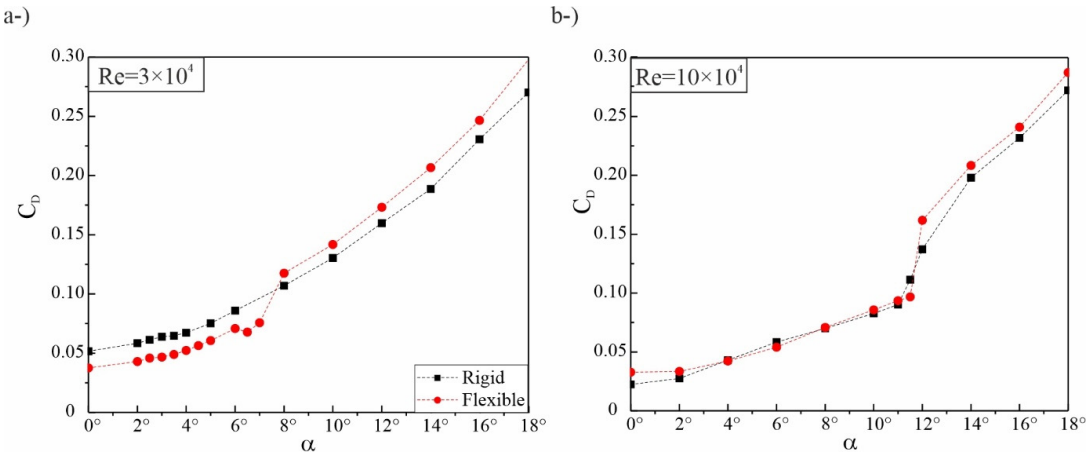

Figure 5. Distribution of C_D for rigid and flexible wing at Re=3×10^4 and 10×10^4.

In order to better compare the aerodynamic performance of rigid and flexible wings at Re=3×10^4 and 10×10^4, the lift to drag variation (C_L/C_D) with angle of attack is illustrated in Figure 6. Figure 6a demonstrated that flexibility significantly improve aerodynamic performance of wing at Re=3×10^4. Specifically, C_L/C_D increases up to α=7° for flexible wing. The maximum value of C_L/C_D is about 7.9 for the flexible wing, while it reaches approximately 1.6 for the rigid wing in the pre-stall region. Moreover, the angle of maximum C_L/C_D is delayed from 2.5° to 7°. A sharp decrease occurs at α=10° due to stall for flexible wing. Beyond this angle, the C_L/C_D value approaches that of the rigid wing due to the increased drag and decreased lift in the post-stall region. The flexible wing can provide a more significant C_L/C_D when Reynolds number increased from Re=3×10^4 to 10×10^4. On the other hand, the flexible wing exhibits nearly similar aerodynamic performance with the rigid wing at Re=10×10^4. The maximum C_L/C_D equals to 10 at α=6°.

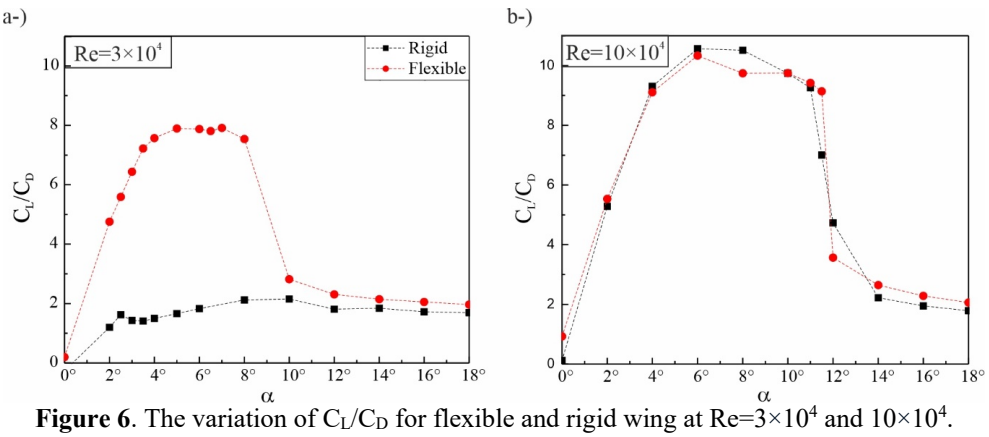

Figure 6. The variation of C_L/C_D for flexible and rigid wing at Re=3×10^4 and 10×10^4.

4. CONCLUSION

This study present experimental investigation in the wind tunnel in order to reveal the effect of flexible surface on the aerodynamic performance of NACA0018 finite wing at low Reynolds numbers. Aspect ratio of wing was kept constant as 4. Force measurement results indicate that flexible wing significantly improve aerodynamic performance at Reynolds number of 3×10^4. Stall is postponed by about 5° when compared to the rigid wing. Furthermore, maximum value of lift coefficient increased by 570% in comparison with rigid wing at $Re=3\times10^4$. On the other hand, the flexible wing has an insignificant effect on aerodynamic performance at $Re=10\times10^4$, as the variations in drag and lift coefficients across different angles of attack are nearly identical to those of the rigid wing. Surface oil flow visualization experiments reveal that the laminar separation bubble dominates the upper surface flow structure at moderate angles of attack, whereas the tip vortex becomes more dominant at $Re=10\times10^4$. In the light of obtained results, the improved performance of the NACA0018 finite wing with a flexible surface is expected to enhance energy efficiency and maneuverability for micro unmanned air vehicles (MUAVs).

5. ACKNOWLEDGEMENT

This study was supported by Scientific and Technological Research Council of Turkey (TUBITAK) under Grant Number 223M340. The authors thank to TUBITAK for their supports.

6. REFERENCES

1. Açıkel, H.H. & Genç, M.S. (2018). Control of laminar separation bubble over wind turbine airfoil using partial flexibility on suction surface. *Energy*, *165*, 176-190.
2. Guo, Q., He, X., Wang, Z. & Wang, J. (2021). Effects of wing flexibility on aerodynamic performance of an aircraft model. *Chinese Journal of Aeronautics*, *34*(9), 133-142.
3. Genç, M.S., Açıkel, H.H. & Koca, K. (2020). Effect of partial flexibility over both upper and lower surfaces to flow over wind turbine airfoil. *Energy Conversion and Management*, *219*, 113042.
4. Koca, K., Genç, M.S., Bayır, E. & Soğuksu, F.K. (2022). Experimental study of the wind turbine airfoil with the local flexibility at different locations for more energy output. *Energy*, *239*, 121887.
5. Demir, H. & Genç, M. S. (2017). An experimental investigation of laminar separation bubble formation on flexible membrane wing. *European Journal of Mechanics - B/Fluids*, *65*, 326–338. https://doi.org/10.1016/j.euromechflu.2017.05.010
6. Lian, Y., & Shyy, W. (2007). Laminar-Turbulent Transition of a Low Reynolds Number Rigid or Flexible Airfoil. *AIAA Journal*, *45*(7), 1501–1513. https://doi.org/10.2514/1.25812
7. Yavuz, M.M. (2021). Flow and mechanical characteristics of a modified naca wing geometry. *Çukurova Üniversitesi Mühendislik Fakültesi Dergisi*, *36*(3), 815-825.
8. Tangöz, S. (2024). Investigation of surface flow behaviors on wing model made of different airfoils. *Çukurova Üniversitesi Mühendislik Fakültesi Dergisi*, *39*(3), 759-770.
9. Shang, H., Wang, Z., Du, L., Wang, Y. & Sun, X. (2024). Experimental and numerical investigations to the aeroelastic response of flexible thin airfoil. *Physics of Fluids*, *36*(6), 067133.
10. Lone, M. & Cooke, A. (2014). Review of pilot models used in aircraft flight dynamics. *Aerospace Science and Technology*, *34*, 55-74.
11. Kang, W., Zhang, J., Lei, P. & Xu, M. (2014). Computation of unsteady viscous flow around a locally flexible airfoil at low Reynolds number. *Journal of Fluids and Structures*, *46*, 42-58.
12. Lei, P.-F., Zhang, J.-Z., Kang, W., Ren, S. & Wang, L. (2014). Unsteady Flow Separation and High Performance of Airfoil with Local Flexible Structure at Low Reynolds Number. *Communications in Computational Physics*, *16*(3), 699-717.
13. Boughou, S., Batistić, I., Omar, A., Cardiff, P., Inman, D.J. & Boukharfane, R. (2024). Investigation on aeroelasticity of morphing wing through dynamic response and virtual structural damping. *Physics of Fluids*, *36*(9), 091902.
14. Roy, A. & Mukherjee, R. (2022). Delay or control of flow separation for enhanced aerodynamic performance using an effective morphed surface. *Acta Mechanica*, *233*(4), 1543-1566.
15. He, X., Guo, Q., Xu, Y., Feng, L. & Wang, J. (2023). Aerodynamics and fluid–structure interaction of an airfoil with actively controlled flexible leeward surface. *Journal of Fluid Mechanics*, *954*, A34.

16. Almalki, H., Safaei, B., Karimzadeh Kolamroudi, M., Sahmani, S., Arman, S. & Shekoofa, O. (2024). Systematic literature review on the design, efficiency and fabrication of wind turbine blades. *International Journal of Ambient Energy*, *45*(1), 2374057.

17. Koca, K., Keskin, S., Şahin, R., Veerasamy, D. & Genç, M.S. (2024). Measurements of Flow Characterization Revealing Transition to Turbulence Associated with the Partial Flexibility-Based Flow Control at Low Reynolds Number. *Arabian Journal for Science and Engineering*.